ures 6 and 7 for comparison with the B-W-R predicted data. Considering that Khazanova et al. attach ± 0.5 atm uncertainty to their reported pressures, there seems to be a reasonable agreement at 10°C. At lower temperatures there is excellent agreement between dew-point pressures measured by Kurata-Swift and those predicted by B-W-R, and reasonable agreement in bubble-point pressures at carbon dioxide concentrations of 40% or more. However, at conditions corresponding to 10 to 20% carbon dioxide in the liquid, bubble-point pressures reported by Kurata-Swift are 1 to 2 atm higher than those measured and correlated in the work presented herein. Consequently, at these conditions the relative volatility of carbon dioxide to ethane implied by the data of Kurata-Swift is about 50% higher than that predicted by B-W-R.

NOTATION

B_0, A_0, C_0, b, a, c, α, γ = pure-component B-W-R coefficients
d = molal density
f = component fugacity
k_{ij} = binary interaction coefficient
K = component equilibrium constant
P = absolute pressure
R = universal gas constant
T = absolute temperature
x = mole fraction of the component in liquid phase
y = mole fraction of the component in vapor phase
Σ = summation term

Subscripts and Superscripts

i, j = total number of components
L = liquid phase
V = vapor phase

LITERATURE CITED

Barner, H. E., and S. B. Adler, "Low Temperature B-W-R Applications," *Hydrocarbon Processing*, **47**, 150 (1968).

Benedict, M., G. B. Webb, and L. C. Rubin, "An Empirical Equation for Thermodynamic Properties of Light Hydrocarbons and their Mixtures," *J. Chem. Phys.*, **8**, 334 (1940).

Benedict, M., G. B. Webb, and L. C. Rubin, "An Empirical Equation for Thermodynamic Properties of Light Hydrocarbons and their Mixtures, Part II. Mixtures of Methane, Ethane, Propane, and *n*-Butane," *ibid.*, **10**, 747 (1942).

———., "An Empirical Equation for Thermodynamic Properties of Light Hydrocarbons and their Mixtures: Constants for Twelve Hydrocarbons," *Chem. Eng. Progr.*, **47**, 419 (1951).

Buell, D. S., and J. W. Eldridge, "Solubility, Vapor Pressure, and Liquid Density in the System Carbon Dioxide-Methylene Chloride," *J. Chem. Eng. Data*, **7**, 187 (1962).

Khazanova, N. E., and L. S. Lesnevskaya, "Phase and Volume Relations in the System Ethane-Carbon Dioxide," *Russ. J. Phys. Chem.*, **41**, 1279 (1967).

Kuenen, J. P., "Experiments on the Condensation and Critical Phenomena of Some Substances and Mixtures," *Phil. Mag.*, **44**, 174 (1897).

Kurata-Swift Consulting Engrs., "Experimental Measurements of Vapor-Liquid Equilibrium for the Ethane-Carbon Dioxide and Nitrogen-n-Pentane Binary Systems," Natural Gas Processors Assoc., Tulsa, Oklahoma, Research Report, RR-5 (Dec., 1971).

Orye, R. V., "Prediction and Correlation of Phase Equilibria and Thermal Properties with the B-W-R Equation of State," *Ind. Eng. Chem. Process Design. Develop.*, **8**, 579 (1969).

Stotler, H. H., and M. Benedict, "Correlations of Nitrogen-Methane Vapor-Liquid Equilibria By Equations of State," *Chem. Eng. Progr. Symp. Ser. No. 6*, **49**, 25 (1953).

Manuscript received June 19, 1973; revision received November 7 and accepted November 8, 1973.

Concentration Profiles in Free-Flow Electrophoresis

An analysis is presented which enables detailed description of solute concentration profiles for free-flow electrophoresis in planar slit flows. This analysis is suitable for either batch or continuous operation with arbitrary variation of solute input rate, and it requires no seriously restrictive assumptions other than constancy of equilibrium and transport properties. It permits for the first time a systematic investigation of the effects of governing parameters and can be used to optimize operating conditions. The most significant finding is that Taylor dispersion, ignored in previous analyses, markedly reduces separability.

JOAQUIM F. G. REIS
E. N. LIGHTFOOT
and
HO-LUN LEE

Department of Chemical Engineering
University of Wisconsin
Madison, Wisconsin 53706

SCOPE

Electrophoresis has become an important analytical tool in protein chemistry because of its excellent resolving power, but it has not proven as successful on a preparative scale. Much developmental effort has been expended to scale up electrophoretic separations, and the reasons for their relative lack of success are not entirely clear. However, the lack of realistic quantitative descriptions of solute distributions has certainly been a major stumbling block. We are attempting to provide improved models as part of an overall design effort, and this paper presents our initial results.

To date the most reliable method for predicting solute separability appears to be the first-order approximation of Philpot (1940) for adiabatic separations in rectangular slit-flow apparatus. Philpot's model predicts that separability depends only upon carrier solvent temperature rise and is completely independent of apparatus shape. It is a quantitative expression of an earlier suggestion by Thomson (1884), and it is useful for orientation purposes. It is, however, a very primitive model which ignores both the nonuniform velocity profiles actually observed as well as spatial variations in fluid density and viscosity.

The parabolic velocity profiles characteristic of slit-flow apparatus produce an axial dispersion analogous to that first studied by Taylor (1953) in tube flow, and this paper deals with their effect in one of the commonest equipment configurations, that of Hannig (1964). Such a system is described schematically in Figure 1.

In such a device solute moves by virtue of the bulk fluid motion $v_x(y)$, that is, by convection, in the x-direction and simultaneously migrates, under the influence of the electric field, in the z-direction. In the absence of diffusion, solute at any y-position would move in a straight line as shown, and the solute as a whole would tend to form a double-valued profile at the end of the apparatus. Resolution of two solutes would be incomplete even in this ideal case.* Diffusion, which is most important in the y- and z-directions, tends to mitigate the extremely rapid migration near the large flat surfaces, but it also interacts with the nonuniform flow to produce an analog of Taylor dispersion. The primary purpose of this paper is to describe quantitatively the combined effects of convection, electro-migration, and diffusion. The immediate benefit of this work is to provide a basis for optimizing equipment configuration and determining the degree to which a given apparatus approaches its separation potential.

This paper is also necessary for examination of hydrodynamic instabilities in electrophoresis. Both uneven heating of carrier solvent and nonuniform distribution of proteins can result in free-convective secondary flows which further reduce separability. These must be considered if one wishes to maximize equipment productivity, and their analysis must start with a precise reliable description of the undisturbed primary flow.

CONCLUSIONS AND SIGNIFICANCE

All the results of this analysis follow directly from Equation (38) which describes the transient concentration profile resulting from introduction of a unit pulse of solute to the apparatus of Figure 1. Profiles for any other schedule of solute addition can be obtained from this fundamental result by superposition, and one of particular importance—steady solute flow—is given by Equation (40). The distribution of solute leaving the apparatus, which directly determines separation effectiveness, is given by Equation (47). Representative numerical results for steady flow are shown in Figures 2, 3, and 4.

Solution of the defining equations for pulse input are surprisingly simple and provide a convenient compact basic description of the system. It may readily be seen from Equation (8) that diffusion in the z-direction and also electrical migration are independent of convection and diffusion in the x and y directions. Furthermore, motion in the x and y directions is described by a two-dimensional analog of Taylor diffusion, most conveniently by extending the analysis of Gill and Sankarasubramanian (1970). The steady result, Equation (40), is inherently more complex.

The possibility of constructing unsteady solutions is particularly attractive for laboratory-scale operations since these are usually carried out on a batch basis. The significance of Equation (39), which is essentially a specialized superposition integral, is then particularly important: the degree of separation of two solutes is the same irrespective of the feed schedule provided that:

1. They are always fed in the same proportion to each other,
2. Their introduction does not affect the flow profiles in the equipment, and
3. Solvent flow is time independent.

The steady state results of Figures 2 to 4 are then also applicable to any transient solute feed schedule.

Most significant numerically is the large effect of Taylor dispersion, not considered in any previous analysis. A specific example, characteristic of commercially available equipment, is shown in Figure 3.

The effects of equipment configuration and operating conditions are shown in Figures 2 to 4. It can be seen from these figures that previous analyses not only underestimated dispersion but were qualitatively incorrect in predicting the effects of changing operating conditions. Thus increasing perfusion and migration velocities in the same ratio is seen to decrease effectiveness of separation substantially whereas the Philpot model predicts an improvement.

Once it is recognized that interaction of nonuniform convection with diffusion is a significant source of dispersion methods can be sought to minimize such interaction. One simple approach which completely eliminates this problem is to operate in a stepwise manner:

1. Feed solute to the apparatus, without an imposed electric field and for a short period such that no substantial amount leaves.
2. Stop convection and apply an electric field for a sufficient time to achieve the desired separation.
3. Elute the solute.

This type of batch operation produces a much more complete separation than can be achieved with continuous flow and is only one example of many possible modifications of the operating procedure suggested by our analysis.

THEORY

Solute profiles are developed in this section for the system of Figure 1: convective flow in the x-direction and electromigration in the z-direction between immobile bounding planes at $y = \pm B$. In the mathematical development these planes are considered to extend indefinitely in the x- and z-directions, but the physical system of interest is that of the figure. In practical situations edge effects at $x = 0$, L and $z = \pm w$ appear to be of little importance.

Problem Statement and Decomposition

The basic solution, for a unit pulse of solute fed, is given in Equation (38), and is obtained from the transient three-dimensional diffusion equation

* Such double-valued concentration profiles have been observed, and described for the nondiffusive limit, by Tippetts et al. (1967). Their model has since been refined by Strickler and Sacks (1973a, 1973b) to include the beneficial effects of electro-osmosis, which had been observed by Grassmann and Hannig (1970).

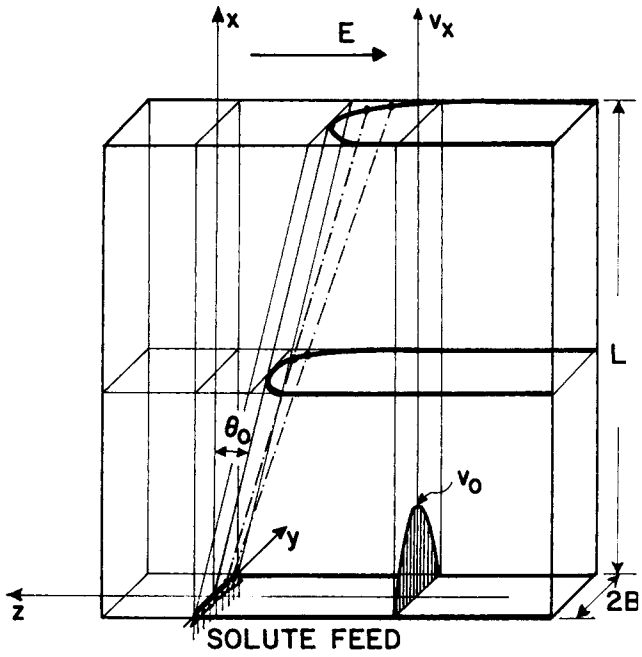

Fig. 1. The system considered. The concentration profiles shown are for the limiting case of zero solute diffusivity. Dashed lines (-.-.-) represent corresponding solute trajectories.

$$\frac{\partial c_i}{\partial t} + v_x \frac{\partial c_i}{\partial x} - \epsilon_0 \frac{\partial c_i}{\partial z} = \mathcal{D}_{im}\left(\frac{\partial^2 c_i}{\partial x^2} + \frac{\partial^2 c_i}{\partial y^2} + \frac{\partial^2 c_i}{\partial z^2}\right) \tag{1}$$

with the aid of the boundary conditions

At	$t = 0$	$c_i = \delta(z)\ \delta(x)$	for $-B \leq y \leq B$	(2)
At	$x = \pm\infty$	$c_i = 0$	for finite t	(3)
		$\partial c_i/\partial x = 0$	for finite t	(4)
At	$y = 0, \pm B$	$\partial c_i/\partial y = 0$		(5)
At	$z = \pm\infty$	$c_i = 0$	for finite x	
		$\partial c_i/\partial z = 0$	for finite x	(6)

The velocity profile is taken as

$$\mathbf{v} = \boldsymbol{\delta}_x\, v_0[1 - (y/B)^2] \tag{7}$$

and v_0, $\mathcal{D}_{im}$, and ϵ_0 are considered to be known constants.

The apparent complexity of Equations (1) to (6) can be much reduced by considering solute motion in the z-direction separately from that in the x- and y-directions, and this is the procedure followed. It is permitted by the linearity of the equations, the simplicity of the boundary conditions on z, and the lack of coupling between these two sets of motions. Mathematically this process may be expressed by setting

$$c_i(x, y, z, t) = \hat{c}(x, y, t)\ g(z, t) \tag{8}$$

with

$$\int_{-\infty}^{\infty} g\,dz \equiv B \tag{9}$$

and

$$\hat{c} \equiv \frac{1}{B}\int_{-\infty}^{\infty} c_i\,dz \tag{10}$$

The choice of B for the integral of g is arbitrary but convenient.

The defining equation for $\hat{c}$ is simply obtained by integrating the basic description with respect to z as indicated by Equation (10). The result is

$$\frac{\partial \hat{c}}{\partial t} + v_x \frac{\partial \hat{c}}{\partial x} = \mathcal{D}_{im}\left(\frac{\partial^2 \hat{c}}{\partial x^2} + \frac{\partial^2 \hat{c}}{\partial y^2}\right) \tag{11}$$

with

At	$t = 0$	$\hat{c} = \delta(x)$		(12)
At	$x = \pm\infty$	$\hat{c} = 0$	for finite t	(13)
		$\partial\hat{c}/\partial x = 0$	for finite t	(14)
At	$y = \pm B$	$\partial\hat{c}/\partial y = 0$		(15)

This is a slit-flow analog of the classic Taylor dispersion problem* (Taylor, 1953); an acceptable approximate solution is given shortly below.

Substitution of Equation (8) into the basic description gives,** with the help of Equation (11),

$$\frac{\partial g}{\partial t} - \epsilon_0 \frac{\partial g}{\partial z} = \mathcal{D}_{im}\frac{\partial^2 g}{\partial z^2} \tag{16}$$

with

$$\text{At}\quad t = 0 \qquad g = \delta(z) \tag{17}$$

$$\text{At}\quad z = \pm\infty \qquad g = 0 \tag{18}$$

This is just the equation for one-dimensional diffusion from a point source with a uniform (electrophoretic) translation at velocity ϵ_0. Since this result is well known we may write immediately

$$g = \frac{B}{\sqrt{4\pi t\,\mathcal{D}_{im}}} \exp\left[-\frac{(z + \epsilon_0 t)^2}{4t\,\mathcal{D}_{im}}\right] \tag{19}$$

Note that g is dimensionless as required by Equation (9).

Solution of the Dispersion Problem

Equation (11) and its attendant boundary conditions describe a slit-flow analog of Taylor dispersion which is important in itself. This equation can be integrated to any desired degree of accuracy† by postulating a solution of the form††

$$\hat{c} = \sum_{n=0}^{\infty} f_n(y, t)\,\frac{\partial^n}{\partial x^n}\,c_m(x, t) \cdot (\mathcal{D}_{im}/v_0)^n \tag{20}$$

with

$$c_m \equiv \int_{-B}^{B} \hat{c}(x, y, t)\,dy \tag{21}$$

It is readily shown from Equation (21) that†††

$$\langle f_0 \rangle = f_0 = 1 \tag{22}$$

and

$$\langle f_n \rangle = 0 \quad (n \geq 1) \tag{23}$$

Furthermore averaging Equation (11) with respect to y yields

$$\frac{\partial c_m}{\partial t} = \sum_{n=1}^{\infty} \beta_n(t)\,\frac{\partial^n c_m}{\partial x^n} \tag{24}$$

with

$$\beta_1 = -\langle v_x \rangle \tag{25}$$

---

* Cox et al. (1972) solved an analogous problem in cylindrical geometry with free convection, in the absence of forced convection.

** Equation (16) may also be obtained by integrating Equation (1) over x and y.

† Within the limitations of the boundary conditions. Equation (3) is physically unrealizable, but order of magnitude estimates suggest that diffusion across the plane $x = 0$ is almost always unimportant.

†† This is a simple generalization of Gill and Sankarasubramanian's approach.

††† $\langle q \rangle \equiv \frac{1}{2B}\int_{-B}^{B} q\,dy$ where q is any function of y.

$$\beta_2 = \mathcal{D}_{im} - \langle v_x f_1 \rangle \left(\frac{\mathcal{D}_{im}}{v_0} \right) \tag{26}$$

$$\beta_n = - \langle v_x f_{n-1} \rangle \left(\frac{\mathcal{D}_{im}}{v_0} \right)^{n-1} \tag{27}$$

It is now convenient to introduce the dimensionless variables

$$X_1 = (x + \beta_1 t)/BP\acute{e} \tag{28}$$

$$\eta = y/B \tag{29}$$

$$\tau = tv_0/B\,P\acute{e} = t\,\mathcal{D}_{im}/B^2 \tag{30}$$

with the Péclet number defined as

$$P\acute{e} \equiv v_0 B/\mathcal{D}_{im} \tag{31}$$

Equation (24) may now be put in the form

$$\frac{\partial c_m}{\partial \tau} = \sum_{n=2}^{\infty} K_n(\tau) \frac{\partial^n c_m}{\partial X_1^n} \tag{32}$$

with

$$K_2(\tau) = \frac{1}{P\acute{e}^2} - \langle v_x^* f_1 \rangle \tag{33}$$

$$K_n(\tau) = - \langle v_x^* f_{n-1} \rangle \quad n > 2 \tag{34}$$

Equations (32) to (34) are closely analogous to the corresponding results of Gill and Sankarasubramanian, and we may continue to parallel their development.

We find that

$$f_1 = \frac{1}{6}\left(\eta^2 - \frac{1}{2}\eta^4 - \frac{7}{30} \right) - 4 \sum_{n=1}^{\infty} \left\{ \frac{(-1)^n}{n^4\pi^4} e^{-n^2\pi^2\tau} \cos n\pi\eta \right\} \tag{35}$$

$$- \langle v_x^* f_1 \rangle = \frac{8}{945} - \frac{8}{\pi^6} \sum_{n=1}^{\infty} \frac{\exp(-n^2\pi^2\tau)}{n^6} \tag{36}$$

where

$$v_x^* = (v_x - \langle v \rangle)/v_0$$

and that from a practical standpoint we may neglect terms for n greater than two in Equation (32). However, it is not reasonable for probable conditions of electrophoresis to neglect the transient terms† in Equation (36).

We may now immediately integrate the truncated form of Equation (32) to obtain

$$\frac{c_m}{c_0} = \frac{1}{\sqrt{4\pi\xi}} \exp(-X_1^2/4\xi) \tag{37}$$

where

$$\xi = \int_0^\tau K_2(\theta)\, d\theta$$

$$c_0 = (M_i/2B^3\,P\acute{e})$$

and M_i is the number of moles of solute species i fed in the pulse.

Equations (37), (33), and (36) provide the basic solution to the dispersion problem to the degree of accuracy normally required. We now return to the description of electrophoresis.

† It is interesting to note in this respect that

$$\lim_{t\to 0} \{K_2\} = 1/P\acute{e}^2 \text{ and } \lim_{t\to 0} \{K_n\} = 0 \text{ for } n > 2$$

All initial dispersion thus results from axial diffusion. An analogous situation, not previously reported, holds for tube flow.

Concentration Profiles

For feed of a unit solute pulse to the apparatus of Figure 1, the concentration profile averaged with respect to y, obtained from Equations (19) and (37), is

$$\frac{\langle c \rangle}{c_0} = \frac{c_m g}{c_0} = \frac{1}{\sqrt{4\pi\xi}} \frac{1}{\sqrt{4\pi\tau}} \exp\left[- \frac{X_1^2}{4\xi} - \frac{\zeta^2}{4\tau} \right] \tag{38}$$

Here

$$\zeta = (z + \epsilon_0 t)/B$$

has been introduced to make all variables dimensionless. The use of both ξ and τ as measures of time is awkward, but unavoidable in view of the probable importance of transients in Equation (36).

For arbitrary solute feed schedules exit concentration profiles can be obtained from Equation (38) by superposition. Thus if solute is fed at a varying mass rate $\dot{M}(t)$ dM/dt, where M is mass fed, the exit concentration is just

$$\langle c_i \rangle = \frac{1}{8\pi B^2 v_0} \int_0^\tau \frac{\exp\left[- \left(\frac{\zeta^2}{4\theta} + \frac{X_1^2}{4\xi} \right) \right]}{\sqrt{\xi\theta}} \dot{M}_i(\tau - \theta)\, d\theta \tag{39}$$

For the case of long-continued solute input at a constant mass rate $\dot{M}$ Equation (39) reduces to

$$\langle c_i \rangle = \frac{M_i}{8\pi B^2 v_0} \int_0^\infty \frac{\exp\left[- \left(\frac{\zeta^2}{4\tau} + \frac{X_1^2}{4\xi} \right) \right]}{\sqrt{\xi\tau}} d\tau \tag{40}$$

This is the steady state solution, applicable for example to the description of Hannig's apparatus. Its significance is shown immediately below.

RESULTS

Here we use the above concentration profiles to provide a relatively convenient approximate description of solute distribution in the exit stream from the apparatus. We then consider some representative numerical examples to illustrate the characteristics of our model and to compare it with previously available analyses.

If M_i is the mass of solute species i fed to the apparatus we are presently interested in the distribution function

$$\phi_i = \frac{1}{M_i} \frac{dM_i}{dz/B}\bigg|_{x=L} = B \int_0^\infty \int_{-B}^{B} N_{ix}|_{x=L}\, dyd\tau \Big/ \int_{-\infty}^{\infty} \int_0^\infty \int_{-B}^{B} N_{ix}\, dyd\tau dz \tag{41}$$

Here ϕ is the fraction of entering solute leaving the apparatus at a position z, per unit dimensionless width in this direction, and N_{ix} is the x-component of the molar solute flux, relative to the apparatus-fixed co-ordinate system of Figure 1.

The solute flux should in principle be determined from Fick's first law

$$N_{ix} = c_i v_x - \mathcal{D}_{im} \frac{\partial c_i}{\partial x} \tag{42}$$

and the appropriate concentration profile, Equations (38), (39), or (40). Fortunately, however, considerable simplification of Equation (41) is normally possible.

First, it may be seen from the linearity of the defining equations that ϕ_i will be independent of the solute feed

schedule. It is therefore most convenient to work with the steady state profile, Equation (40), where the integration with respect to time has already been performed. For this situation

$$\phi_i = \frac{1}{\dot{M}_i}\frac{d\dot{M}_i}{dz/B} \tag{43a}$$

$$= \frac{B}{\dot{M}_i}\int_{-B}^{B} N_{ix}|_{x=L}\, dy \tag{43b}$$

It now remains only to obtain a satisfactory approximation for the molar flux.

For most if not all configurations of practical interest it appears that the axial diffusion term, underlined in Equation (42), is of negligible importance. Then

$$\phi_i = \frac{2}{\dot{M}_i} B^2 \langle c_i v_x \rangle \tag{44}$$

to an excellent approximation. This expression in turn may be conveniently expressed as

$$\phi_i = 2\alpha \frac{B^2\langle v\rangle}{\dot{M}} \langle c_i \rangle \tag{45}$$

where

$$\alpha \equiv \langle c_i v_x\rangle / \langle c_i\rangle\langle v\rangle \tag{46}$$

may be determined with the aid of Equation (35). Normally, however, α will vary little with time, position, or species and will not be far from unity. We may then approximate Equation (45), with the aid of Equation (40), as*

$$\phi_i = \frac{1}{6\pi}\int_0^\infty \frac{\exp\left[-\left(\frac{\zeta^2}{4\tau} + \frac{L_1^2}{4\xi}\right)\right]}{\sqrt{\xi\tau}}\, d\tau \tag{47}$$

Here $L_1 = (L + \beta_1 t)/BP\acute{e}$. Equation (47) provides an excellent basis for estimation of separability of two or more solutes. The primary effect of omitting α is that integrals of the ϕ_i over ζ will differ somewhat from unity.

Equation (47) completes our development. It differs substantially from the earlier result of Philpot

$$\phi_i(\text{Philpot}) = \frac{1}{\sqrt{4\pi\dfrac{\mathcal{D}_{im}x}{\langle v\rangle B^2}\cdot\dfrac{\langle v\rangle}{\sqrt{\langle v\rangle^2+\epsilon_0^2}}}} \exp\left[-\left(\frac{z}{B} + \frac{x}{B}\cdot\frac{\epsilon_0}{\langle v\rangle}\right)^2 \Big/ \left(4\frac{\mathcal{D}_{im}x}{\langle v\rangle\cdot B^2}\cdot\frac{\langle v\rangle}{\sqrt{\langle v\rangle^2+\epsilon_0^2}}\right)\right] \tag{48}$$

which does not consider the effect of the nonuniform velocity profile. To show the importance of this previously neglected effect, we give in Figures 2 to 4 the results of numerical calculation for the following representative conditions:

Geometry:

$$L = 1,\ 10,\ 30 \text{ cm}$$

$$2B = 2,\ 8 \text{ mm}$$

Electric field,

$$E = 1,\ 5 \text{ volts/cm}$$

Velocity,

$$v_0 = 1,\ 5 \times 10^{-4} \text{ cm/s}$$

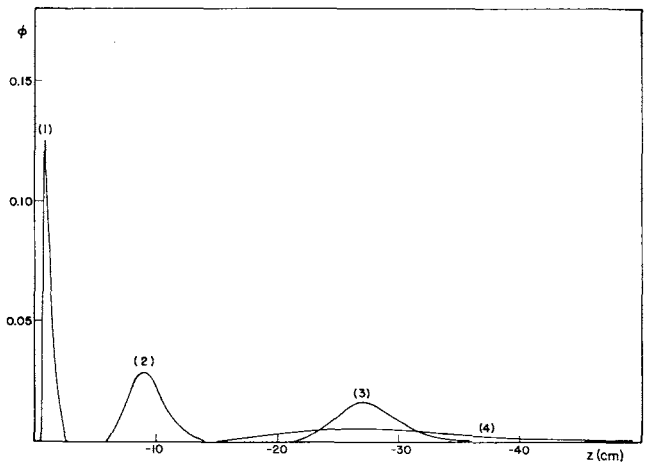

Fig. 2. Effect of geometry on solute distribution. Each curve is drawn for $P\acute{e} = 100$ and $(\epsilon_0/v_0) = 0.6$. Curves (1), (2), and (3) are drawn for $B = 1$ mm and $L = 1$ cm, 10 cm, and 30 cm, respectively. Curve (4) is for $B = 4$ mm and $L = 30$ cm.

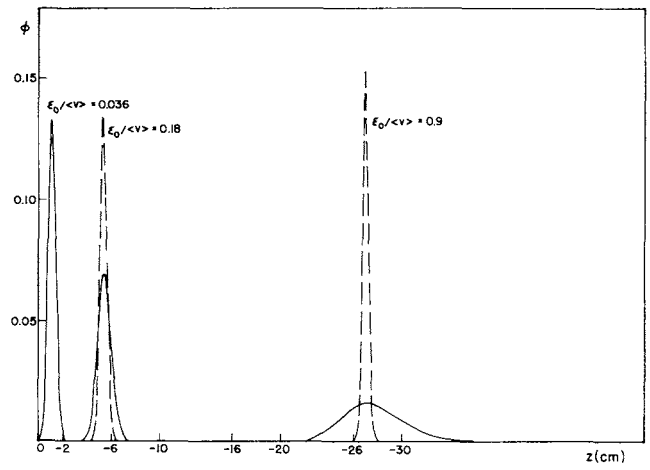

Fig. 3. Effect of solute trajectory on dispersion. Each curve is drawn for $P\acute{e} = 100$, $B/L = 3.3 \times 10^{-3}$, and a cell length of 30 cm. However, the values of (ϵ_0/v_0) vary as shown.

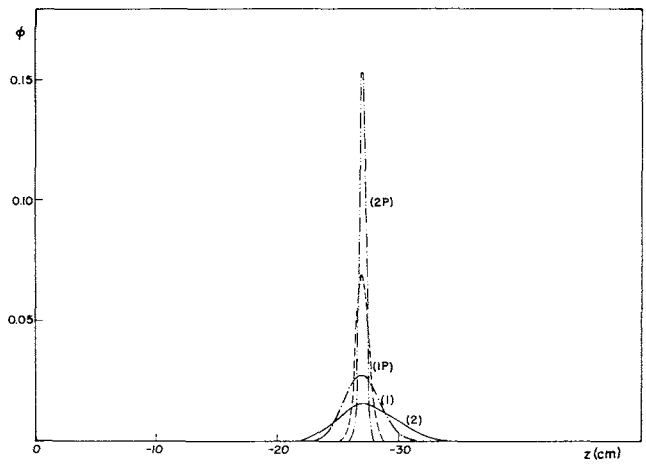

Fig. 4. Effect of Péclet number on dispersion. Each curve is drawn for $(\epsilon_0/v_0) = 0.6$, $(B/L) = 0.00333$, and $L = 30$ cm. However, curves 1 and 1P are for $P\acute{e} = 20$ and curves 2 and 2P for $P\acute{e} = 100$. Curves 1 and 2 are calculated from our model; 1P and 2P from that of Philpot.

* Note that $\langle v\rangle = \frac{2}{3} v_0$.

Solute:

$\mathcal{D}_{im}$ 5×10^{-7} cm²/s

$\mu_i = \epsilon_0/E$ 6×10^{-5} cm²/volt, s

Here μ_i is electrophoretic mobility of species i. The solute is hypothetical, but similar to serum albumin.

Figure 2 was constructed to show the effect of geometry and covers the above-indicated range of conditions. Curves (1), (2), and (3) show the increasing dispersion occurring as cell length is increased from one to thirty centimeters for $B = 1$ mm. Curves (3) and (4) show the very large increase in dispersion resulting when B is increased from one to four millimeters at $L = 30$ cm. It may also be noted that the marked asymmetry of curve (4) results in a substantial leftward shift of the concentration maximum. It can be seen from these results that changing the plate spacing $2B$ has a more profound effect than changing cell length L.

In some respects, however, Figure 2 is misleading, and a plot of $(\phi L/B)$ versus z/L would give somewhat different insight. In such a plot concentration peaks would approximately coincide, and those for greater L would be higher. Since the areas under the curves would all be the same this means that a relatively sharper separation is obtained in longer cells. Such behavior is qualitatively the same as that predicted by the Philpot model, and to a first approximation it has the same basis as given by Philpot: dispersion increases only (approximately) as the square root of time whereas lateral displacement is exactly proportional to time for each solute molecule. In other respects, however, the Philpot model is a poor guide, and this is shown in the last two figures.

Figure 3 compares solute profiles for the present model with those of Philpot for three different trajectory parameters (ϵ_0/v_0), and it shows clearly the major defect of the earlier model: neglect of Taylor dispersion. For vanishingly small migration velocities such dispersion has little effect laterally, and for $(\epsilon_0/v_0) = 0.036$ the two models are indistinguishable to the precision shown. However, the present treatment shows that lateral dispersion increases markedly with increase in migration velocity. The Philpot model, on the other hand, incorrectly predicts an improvement and therefore suggests nonbeneficial changes in equipment design.

Separability depends only upon dispersion relative to mean displacement and the ratio of these is not greatly different for (ϵ_0/v_0) of 0.18 and 0.9. However, relative dispersion is larger for $(\epsilon_0/v_0) = 0.036$ and for very large (ϵ_0/v_0). There is then an optimum (ϵ_0/v_0) for separability, and it is inadvisable to use very large migration velocities. There may also be an optimum from the standpoint of power consumption, but we have not yet investigated this.

The importance of considering Taylor dispersion is further emphasized in Figure 4 where dispersion is shown to increase with an increase in Péclet number. For these conditions the opposite effect (and much smaller dispersion) are predicted by the simpler model.

In summary then we find that system behavior is profoundly influenced by Taylor dispersion, which must therefore be taken into account. Its effects are actually more complex than indicated by the last three figures, and the model presented here deserves extensive study. However, it appears to indicate that small (B/L) are highly desirable and that large (ϵ_0/v_0) are at best not useful. These facts alone provide useful insight, and our model seems adequate to describe free-flow electrophoresis at vanishingly small solute concentrations and current densities.

Since maximizing equipment productivity requires both finite solute concentrations and high current densities, however, it is clearly necessary to look at free convection and hydrodynamic stability. This is our next objective.

ACKNOWLEDGMENTS

The authors are indebted for financial support to the National Science Foundation Grant GK33346X. In addition, J. F. G. Reis wishes to acknowledge assistance provided by Fundação Calouste Gulbenkian (Portugal) Fellowship.

NOTATION

B = half thickness of cell, l

c_i = molar concentration of solute species i, m/l^3

$\hat{c}$ = concentration averaged with respect to z

c_m = concentration averaged over the y-z plane

$c_0 = M_i/2B^3Pé$

$<c>$ = concentration averaged with respect to y

$\mathcal{D}_{im}$ = effective binary diffusivity of species i, l^2/t

E = electric field strength, volts/cm

f_i = dimensionless functions defined by Equation (20)

L = cell length, l

$L_1 = (L + \beta_1 t)/BPé$, dimensionless

M_i = number of moles of i fed to apparatus, m

M_i = moles of i fed per unit time, m/t

$Pé = Bv_0/\mathcal{D}_{im}$ = Péclet number, dimensionless

t = time

$v_x = v_0[1 - (y/B)^2]$ = x-component of fluid velocity, l/t

$v_x^* = (v_x - <v>)/v_0$, dimensionless

v_0 = maximum velocity

$<v>$ = v_x averaged over y

w = width of cell, l

x = coordinate in direction of flow, l

$X_1 = (x + \beta_1 t)/BPé$

y = coordinate perpendicular to confining plates, l

z = coordinate in direction of electric field, l

$\alpha = <c_i v_x>/<c_i><v_x>$

β_n = dispersion coefficient, as defined in Equations (25) to (27)

$\delta(u) = 0, u \neq 0; \int_{-\infty}^{\infty} \delta du = 1$; dimensionless

δ_i = unit vector in i-direction, dimensionless

$\epsilon_0 = E\mu_0$ = electrophoretic velocity, l/t

$\zeta = (z + \epsilon_0 t)/B$, dimensionless

$\eta = y/B$, dimensionless

μ_i = electrophoretic mobility of species i, l^2/t-volts

$\xi = \int_0^\tau K_2(\theta)\, d\theta$, dimensionless

$\tau = t\,\mathcal{D}_{im}/B^2$, dimensionless

ϕ_i = dimensionless solute distribution defined by Equation (41)

LITERATURE CITED

Cox, H. C., J. K. C. Hessels, and J. M. G. Teven, "On the Efficiency of Gel Electrophoresis," *J. Chromatogr.*, **66**, 19 (1972).

Gill, W. N., and R. Sankarasubramanian, "Exact Analysis of Unsteady Convective Diffusion," *Proc. Roy. Soc.*, **A316**, 341 (1970).

Grassmann, W., and K. Hannig, German Patent number 1,442,416 "Continuous Carrier-Free Vertical Electrophoresis" (Cl. B01d) (1970).

Hannig, K., "Eine Neuentwicklung der trägerfreien kontinuierlichen Elektrophorese," *Z. physiol. chem.*, 338, 211 (1964).

Philpot, J. St. L., "The Use of Thin Layers in Electrophoretic Separation," *Trans. Faraday Soc.*, 36, 38 (1940).

Strickler, A., and T. Sacks, "Continuous Free-Film Electro-

phoresis: The Crescent Phenomenon," *Prep. Biochem.*, 3, 269 (1973a).
———., "Focusing in Continuous-Flow Electrophoresis Systems by Electrical Control of Effective Cell Wall Zeta Potentials," *Ann. N. Y. Acad. Sci.*, **209**, 497 (1973b).
Taylor, G. I., "Dispersion of Soluble Matter in Solvent Flowing Slowly through a Tube," *Proc. Roy. Soc.*, **A219**, 186 (1953).
Thomson, W., "Mathematical and Physical Papers" *Vol. II, Sec. VIII*, 46 (1884).
Tippetts, R. D., H. C. Mel, and A. V. Nichols, in "Chemical Engineering in Medicine and Biology," D. Hershey (edit)., p. 505, Plenum Press, N. Y. (1967).

Manuscript received August 15, 1973; revision received December 10 and accepted December 20, 1973.

An Effective Numerical Integration Method for Typical Stiff Systems

There is an equivalence between stiff and singularly perturbed systems of ordinary differential equations. This feature is exploited in this paper by numerically employing recent singular perturbation methods to attack troublesome boundary layer stage of the solution in which some variables have very short response times. The numerical method affords a means of essentially determining the thickness of this boundary layer. The algorithm is capable of high stability and accuracy for the commonly occurring stiff system, whether or not it is in singularly perturbed form. Application to a singularly perturbed reaction system and a highly stiff reactor system not in singularly perturbed form demonstrate the effectiveness and utility of this approach.

RICHARD C. AIKEN and LEON LAPIDUS

Department of Chemical Engineering
Princeton University
Princeton, New Jersey 08540

SCOPE

Many commonly occurring physical and chemical dynamic systems have widely separated time constants. These systems are often represented by sets of initial-value ordinary differential equations which possess variables that rapidly change during time intervals much smaller than the duration of the phenomenon of interest (Lapidus et al., 1973). This presents the numerical integration difficulties associated with such stiff systems. Thus even integration routines stable for any step size (so-called "A-stable" methods) have accuracy problems in following the eigenvalues large in absolute value which damp out early in the solution. This error can easily propagate to destroy the remainder of the transient.

It is of major importance that the practitioner be able to identify the occurrence of a stiff problem. Otherwise, confusion can arise as to why the commonly available integration routines require inordinately small step sizes to obtain an insignificant fraction of the transient (at great expense in computation time). Even when the nature of the difficulty is realized, the popular decision to turn to complex analytical asymptotic methods (MacMillan, 1968) or pseudo steady state hypotheses (Gelinas, 1972) must be viewed with caution as the degree of error introduced is unknown. A number of viable alternatives for the direct numerical integration have been emerging rather recently, however (Lapidus et al., 1973; Seinfeld et al., 1970), and knowledge of these would prove valuable to the general user.

The present study, based on an extension of Miranker (1972), offers one such technique capable of high numerical stability and accuracy. It is particularly effective for systems having some variables with very short initial response times, as frequently occurs within chemical engineering contexts.

Details of the numerical algorithm are presented here as well as the use of the algorithm for two examples of direct interest to the chemical engineer. These examples are the thermal decomposition of ozone and the dynamic behavior of a catalytic fluidized bed. Many other stiff problems are also identified.

CONCLUSIONS AND SIGNIFICANCE

Recognition of the equivalence of stiff and singularly perturbed equations makes available new tools for the solution of both forms of equations. In this study, use is made of singular perturbation methods to develop a numerical technique capable of high stability and accuracy. A unique feature present is the ability to monitor the contribution of the stiff component to assess when the solution is out of the boundary layer. Thereafter the bulk of the transient may be obtained without the accuracy problems associated with this initial section. The numerical approach is applicable to numerous problems in chemical engineering and other disciplines where currently inadequate solution procedures are employed.